ELSEVIER

Journal of Chromatography B, 695 (1997) 15–25

JOURNAL OF CHROMATOGRAPHY B

Pulsed electrochemical detection of thiols and disulfides following capillary electrophoresis

George S. Owens, William R. LaCourse*

Department of Chemistry and Biochemistry, University of Maryland Baltimore County, 1000 Hilltop Circle, Baltimore, MD 21250, USA

Abstract

Pulsed electrochemical detection (PED) following capillary electrophoresis (CE) has been applied to the direct detection of thiocompounds. Both reduced and oxidized thiol moieties are detected without the need of derivatization. Thiocompounds can be detected over a wide range of pH conditions (i.e., pH 0–14), and except for pH, their response is relatively unperturbed by buffer composition. Integrated pulsed amperometric detection (IPAD) results in more stable baselines, eliminates oxide-induced artifacts, and yields lower limits of detection than other PED waveforms. Mass detection limits using optimized IPAD waveforms are typically 2 pg (5 fmol) or less. The high selectivity of PED for thiocompounds reduces sample preparation and produces simpler electropherograms of complex samples containing these biologically significant compounds.

Keywords: Thiols; Disulfides; Thiocompounds

1. Introduction

Numerous thiocompounds play important roles in biological systems. Sulfur-containing amino acids (i.e., cysteine, methionine) are important building blocks of peptides and proteins. Glutathione acts as an intracellular reductant, participates in the transfer of certain amino acids across membranes in the kidney, and assists in the metabolism of potentially toxic xenobiotics [1,2]. Critically important to one's health are exogeneous compounds, such as penicillins and cephalosporins, which fight and eliminate infections and disease. Hence, thiocompounds and related analogues must often be determined in complex biological matrices.

The ability to resolve complex mixtures is greatly facilitated by capillary electrophoresis (CE). The high separation efficiency of CE results in very narrow electrophoretic bands derived from small sample volumes (i.e., <100 nl). Inherently due to the small diameter of the capillary tube (i.e., <100 μm I.D.), optical detection of compounds with weak extinction coefficients (e.g., thiols) results in poor sensitivity and high limits of detection. Hence, the direct detection of aliphatic thiocompounds poses a challenging analytical problem.

Since electrochemical detection (ED) is based upon a reaction at an electrode surface, the electrode and the associated detector cell volume can be made very small with no adverse effects on sensitivity [3]. Several papers have utilized d.c. amperometry at solid electrodes (e.g., Hg/Au amalgam, cobalt phthalocyanine, mixed-valence RuO-CN modified) to detect thiocompounds with high sensitivity. Limits of detections for thiols typically range from 0.03 to 5 μ*M* at Hg/Au amalgam [4] and cobalt phthalo-

*Corresponding author.

PII S0378-4347(97)00096-0

cyanine [5,6] electrodes. Unfortunately, these electrodes can not detect disulfides directly. Dual electrode systems [7], which work well in liquid chromatography, are difficult to implement in microseparation techniques. Application to CE has resulted in compromised limits of detection for disulfides (i.e., 100 μM for cystine). Modified electrodes [8] have fared better for disulfides (i.e., 2–6 μM for thiols and disulfides), but these electrodes have a limited usable lifetime and are subject to pH limitations. More recently, pulsed electrochemical detection (PED) has been applied to the direct and sensitive detection of polar aliphatic compounds (e.g., carbohydrates, amino acids and thiocompounds) following CE [9–12]. PED at noble metal electrodes exploits surface-catalyzed oxidations of various functional groups via potential–time (E–t) waveforms, which combine amperometric detection with alternated anodic and cathodic polarizations to clean and reactivate the electrode surface [13–15]. Sulfur-containing compounds are detected via an oxide-catalyzed mechanism, and LaCourse and Owens [16] determined that integrated pulsed amperometric detection (IPAD) following CE is better suited to manage the large oxide-formation background, which is concomitant with the anodic response of thiocompounds. The IPAD waveform (Table 1) utilizes a potential scan in the detection step which coulometrically rejects the substantial oxide formation signal. IPAD produces more stable baselines, eliminates oxide-induced artifacts, and often yields lower limits of detection than other PED waveforms.

In this paper, electrochemical characterization via cyclic and pulsed voltammetry [17] forms the basis of optimization of IPAD waveforms of thiols and, especially, disulfides at microelectrodes. The analytical figures of merit for PED following electrophoretic separations are determined for model com-

Table 1
Optimal IPAD waveform parameters

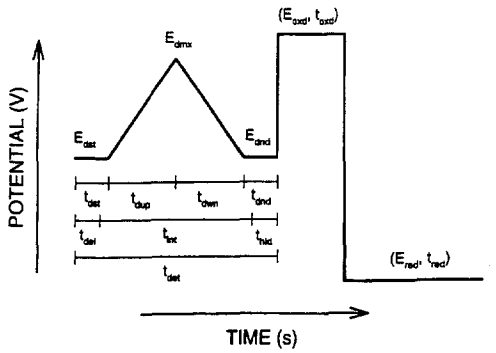

Parameter	Potential (V vs. Ag/AgCl)	Parameter	Time (ms)
E_{dst}	−0.40	t_{dst}	0
E_{dmx}	+1.60	t_{dup}	250
		t_{dwn}	250
E_{dnd}	−0.40	t_{dnd}	0
		t_{det}	500
		t_{del}	0
		t_{int}	500
		t_{hld}	0
E_{oxd}	+1.50	t_{oxd}	100
E_{red}	−1.10	t_{red}	100

pounds. Electropherograms are used to illustrate the wide range and applicability of CE–IPAD to biological compounds of critical significance.

2. Experimental

2.1. Reagents

All analytes and chemicals were reagent grade obtained from Sigma (St. Louis, MO, USA), Aldrich (Milwaukee, WI, USA), or Fisher Scientific (Pittsburgh, PA, USA) and were used without further purification. Stock analyte solutions were either prepared fresh daily or stored under refrigerated conditions. All solutions were filtered with 0.2-μm filters (Rainin, Woburn, MA, USA) and a solvent filtration apparatus (Microfiltration Systems, Rainin). Water was purified using a reverse-osmosis system coupled with multi-tank/ultraviolet/ultrafiltration stations (U.S. Filter/IONPURE, Lowell, MA, USA).

2.2. Apparatus

2.2.1. Voltammetry

Cyclic voltammetric data were obtained at Au microelectrodes (ca. 12 μm O.D.) using a Model BAS-100 electrochemical analyzer (Bioanalytical Systems (BAS), West Lafayette, IN, USA). For all experiments a Pt auxiliary electrode was used. All potentials are reported versus a Ag/AgCl reference electrode (Model MW-202, BAS). The electrochemical cell (ca. 15 ml) was constructed of Pyrex glass.

Pulsed voltammetry (PV) was accomplished using a computer-controlled potentiostat (Model AFRDE-5; Pine Instrument, Grove City, PA, USA) interfaced to a 486/33 MHz IBM-compatible computer via a DAS-1600 high-speed AD/DA expansion board (Keithley Data Acquisition, Taunton, MA, USA). Pulsed voltammetric waveforms were generated with ASYST Scientific software (Asyst Software Technologies, Rochester, NY, USA).

2.2.2. Capillary electrophoresis

The CE system with electrochemical detection is based upon a design by O'Shea et al. [18]. Electrophoresis in the capillary was driven by a Model CZE 1000R high-voltage power supply (Spellman Electronics, Plainview, NJ, USA). Polyimide-coated fused-silica capillary columns of 360 μm O.D. and 50 μm I.D. were obtained from Polymicro Technologies (Phoenix, AZ, USA). Sample introduction was accomplished electrokinetically using a laboratory-made timer, which controlled the high-voltage power supply.

The decoupler, which introduces a controlled fracture into the capillary tubing ca. 2 cm from the end, is used to drop the electrophoretic potential to near zero before the electrochemical detection cell. The decoupler does not interfere with the electroosmotic flow of the CE system. Typically, the potential drop between the decoupler and the electrochemical cell is approximately one volt. The decoupler design has been described in detail elsewhere [19]. The junction was covered with either Nafion tubing or coated with liquid Nafion (Sigma), which was allowed to dry while air pressure from a 50-ml disposable syringe was applied to the capillary.

The outlet capillary (ca. 2-cm) of the decoupler was inserted through the wall of a ca. 10-ml rubber septum (Fisher). This reservoir served as the electrochemical cell. A three-electrode configuration was used. The working electrode was a Au microelectrode, which was inserted into the capillary using a Model N39,361 stereo microscope (Edmund Scientific, Barrington, NJ, USA). A Ag/AgCl reference electrode and a Pt auxiliary electrode were used for all CE–PED experiments. The entire decoupler/destination–electrochemical cell was placed in a metal enclosure, which acted as a Faraday cage.

Gold microelectrodes were fabricated by bonding a 1-cm length of 12 μm O.D. Au wire (Alfa Products, Johnson-Matthey, Ward Hill, MA, USA) to 0.125 mm O.D. copper wire with conductive silver paint (Ladd Research Industries, Burlington, VT, USA). The Au wire/Cu wire assembly was inserted into a 1.59 mm O.D. glass tube, which had been pulled to a point in a Bunsen burner flame. The Au wire protruded from the tip of the glass tube. The tube was then filled with a UV-curing epoxy, which sealed the assembly into the glass tube. After curing the Au fiber was trimmed to ca. 0.5 mm with surgical scissors. Approximately 0.2 mm of the

microelectrode was inserted into the capillary for end-column detection.

2.2.3. Pulsed electrochemical detection

Pulsed electrochemical detection at Au microelectrodes was accomplished using the computer-controlled potentiostat described in Section 2.2.1. PAD and IPAD waveforms were generated with ASYST Scientific software (Asyst).

2.2.4. Separation conditions

For the CE separations, a capillary length of 50 cm with a voltage of 11 kV was employed unless otherwise noted. The run buffers were typically 10 m*M* phosphate (pH 7.0 or 6.3) adjusted with NaOH pellets (Aldrich). The buffer was prepared from HPLC grade H_3PO_4 (Fisher), which results in smoother baselines.

2.3. Procedures

All pulsed voltammetric experiments were performed with the Au fiber working electrode inserted into the end of a capillary-decoupler system identical to that used for separations. An electrophoretic potential of 11 kV was applied to drive analyte transport to the detection cell during a PV experiment.

3. Results and discussion

It is important to note that PED exploits electrocatalyzed oxidations at noble metal electrodes, and, as a consequence, PED is class (i.e., functional group) specific and not compound specific. Hence, the voltammetric response characteristics and optimized PED waveform under a particular pH and electrolyte composition are universally applicable to essentially all compounds within a compound's class.

The model compounds studied were chosen to represent a wide range of sulfur-containing compounds of biological significance. Fig. 1 shows the molecular structure of these compounds which include thiols (i.e., cysteine, glutathione), disulfides (i.e., dithiane, cystine, glutathione disulfide) and thioethers (e.g., methionine, biotin, penicillin-G and related β-lactams). In the majority of cases, the strong adsorption characteristics of sulfur-containing functional groups dominate the electrochemical response profile of a compound. These compounds reflect a wide range of electrochemical adsorption characteristics.

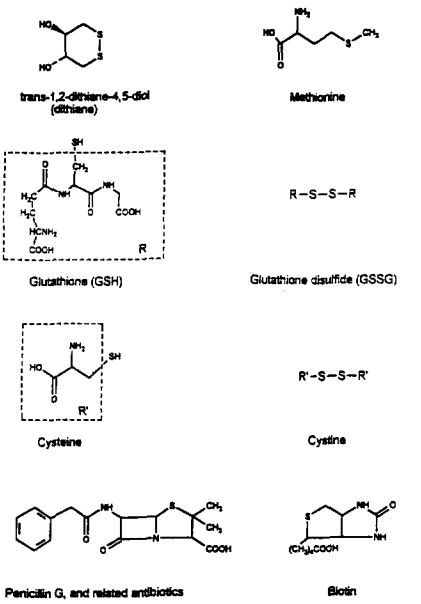

Fig. 1. Chemical structures of various thiocompounds relevant to this study.

3.1. Electrochemical response of selected sulfur compounds

Since the detection step of the IPAD waveform contains a cyclic potential scan which takes place in a short period of time, the scan rates are relatively high (i.e., >1000 mV s^{-1}). It was previously determined that smaller diameter electrodes (i.e., <100 μm O.D.) minimize deleterious effects which are dependent upon scan rate [16,19]. These effects include smearing of the Au oxide formation/dissolution signal due to a combination of increased capacitive currents, uncompensated iR drop, and slow heterogeneous kinetics of oxide formation and dissolution. In other words, the use of small diameter electrodes allows for the use of faster scan rates, which are critical to the effective implementation of IPAD in CE for the preservation of separation

efficiency by using high frequency waveforms. Hence, for all the experiments in this paper, a 0.65 mm×12 μm diameter Au fiber electrode was chosen to maximize the signal-to-noise ratio (S/N) while allowing for the use of fast scan rates.

The current–potential (i–E) response is shown in Fig. 2A for a Au fiber electrode in 10 mM phosphate buffer, pH 7.0 for (-···-) GSH and (——) dithiane in the presence of dissolved O_2. The residual response for the supporting electrolyte (·····) exhibits anodic waves on the positive scan in the regions of ca. +650 to +1400 mV (wave a) for oxide formation and E>1400 mV (wave b) for O_2 evolution.

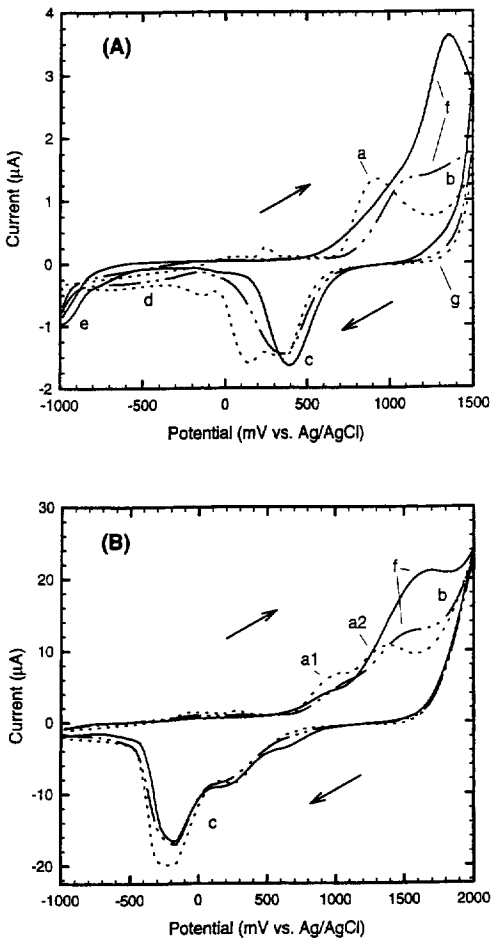

Fig. 2. Voltammetric response at scan rates of (A) 2000 and (B) 25 000 mV s^{-1} at a 12 μm Au fiber electrode in 10 mM phosphate buffer (pH 7.0). Solutions (400 μM): (——) dithiane; (-···-) glutathione (GSH); and (·····) residual.

Cathodic peaks are obtained on the negative scan in the region of ca. +700 to + −300 mV (wave c) corresponding to the dissolution of surface oxide formed on the positive scan, ca. −100 to −900 mV (wave d) for the reduction of dissolved O_2, and E<−900 mV (wave e) for H_2 evolution from solvent breakdown.

Both GSH (-···-) and dithiane (——) give anodic waves on the positive scan commencing at ca. +500 mV (wave f). This wave corresponds to oxidation of the thio groups of the respective compounds. Detailed mechanisms of thiol and disulfide oxidations at Au have been published [20–26]. Oxidation of sulfur-containing groups is classified as an oxide-catalyzed detection. Anodic oxygen transfer to the analyte is promoted via the labile hydrous oxide intermediates of the forming surface oxide, and as a consequence, the anodic response of sulfur-containing compounds in coincident with surface oxide formation (wave a). The onset of activity for the disulfide oxidation in dithiane appears to occur at potentials less negative than the apparent wave for oxide formation in the supporting electrolyte. This observation indicates the surface oxide commences to a limited degree in the potential region of ca. +300 to +600 mV. The presence of oxide at these potentials is supported by the small anodic peak at ca. +250 mV, which is attributable to the formation of AuOH at a particular crystal face. This oxide peak is typically not observed at lower scan rates. The anodic signal on the reverse scan in the region of ca. +1500 to +1000 mV (wave g) is indicative of the reactivity of the oxide-covered surface for thio oxidation at constant applied potentials. Virtually all thiols and disulfides behave similarly to GSH and dithiane, respectively.

Sulfur-containing compounds are known to be strongly adsorbed to the electrode surface, and preadsorption of GSH and dithiane is evidenced by the complete suppression of the cathodic reduction wave for dissolved O_2. In addition, the onset of surface oxide formation is also inhibited, altered, or pushed to more positive potentials by the presence of these strongly adsorbing sulfur-containing compounds. Although both compounds alter the anodic wave for oxide formation, GSH shows a much greater effect with an almost 200 mV more positive displacement of the onset of oxide formation, see

Fig. 2A. Although the shape of the oxide formation wave may be different in the presence of strongly adsorbed compounds, the amount of oxide formed remains constant, as supported by the near constant area of the cathodic dissolution peak for both analytes. At lower analyte concentrations typical of an analytical method, the amount of oxide formed in the presence and absence of the analyte has been shown to be virtually the same [16].

The voltammograms in Fig. 2B are similar in all respects to that of Fig. 2A except that the scan rate is 25 000 mV s^{-1} as opposed to 2000 mV s^{-1}. Under these conditions, the absolute signals are for both the analyte and the residual are significantly higher, which is as expected for surface-controlled processes [27]. Since both the analyte and the residual signals are increased proportionally, no analytical advantages are derived from this effect. Interestingly, the anodic response for the residual has now been resolved into two waves (a1 and a2). Multiple peaks such as these have been assigned to the formation of various AuO_xH_y species [28]. It is important to note that the residual and analyte responses are not adversely affected at the higher scan rates. Hence, high frequency IPAD waveforms are possible.

3.2. Optimization of IPAD waveforms

Pulsed voltammetry (PV) [17] has been shown to be the definitive method for characterizing analyte response and optimizing waveform parameters in PAD. In this paper, we have developed a similar computer-controlled method for studying and optimizing IPAD waveforms. The IPAD waveform, see Table 1, was optimized using the "guidelines" outlined in previous publications [13–15]. The scan begins at a potential less than the potential for onset of oxide formation and ends at a potential after which the surface oxide on the forward scan was cathodically dissolved. These potentials were initially chosen to be $E_{dst}=E_{dnd}=-800$ mV.

The maximum scan potential (E_{dmx}) is chosen to encompass the greatest extent of signal under mass-transport control with minimal contribution from the residual scan. Fig. 3 shows the net charge, or background-corrected charge, as E_{dmx} is scanned from +400 to +1800 mV for GSH (▼) and dithiane (●) in phosphate buffer. During this experiment the scan rate is kept constant at 8000 mV s^{-1}, and as a consequence, the integration period (t_{int}) is allowed to increase as needed (see insert in Fig. 3). For both

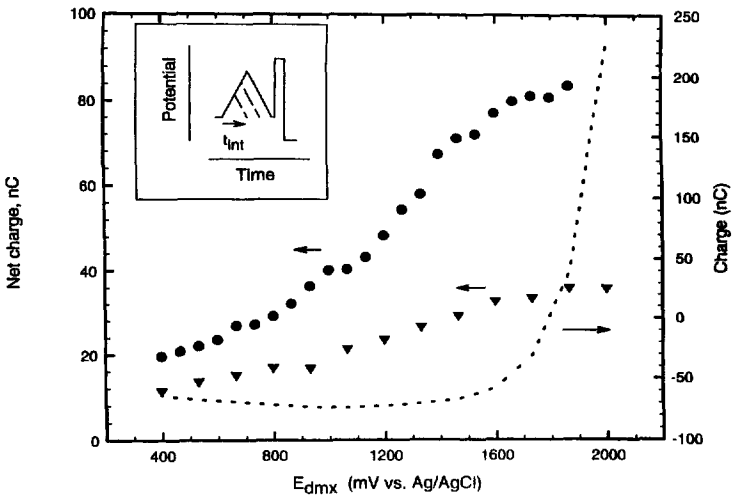

Fig. 3. Pulsed voltammetric background-corrected response as a function of E_{DMX} for thiocompounds at a 12 μm Au fiber electrode in 10 m*M* phosphate buffer (pH 7.0). The inset shows the scheme of PV optimization. Scan rate was fixed at 8000 mV s^{-1} and E_{dmx} was incremented. Solutions (100 μ*M*): (●) Dithiane; (▼) GSH; and (- - -) residual. (inset: scheme of optimization PV scans).

compounds, a plateau is observed at ca. 1600 mV. The plateau for both compounds corresponds to a sharp increase in background charge, which corresponds to the onset of O_2 evolution. The *S/N* results followed the same trend at the net charge, and decayed dramatically with the onset of O_2 evolution at ca. +1750 mV. The optimization of E_{dmx} was also studied by holding t_{int} constant and allowing the scan rate to increase accordingly. Fig. 4A shows the net charge for dithiane as E_{dmx} was scanned from 0 to 2300 mV at t_{int} values of 133 to 600 ms. These show that at every t_{int} value a peak maxima was obtained at 1600 to 1800 mV. As expected, the maximum net charge increases linearly with integration time, Fig. 4B. From these experiments, E_{dmx} was chosen to be +1600 mV, and t_{int} was set to the maximum allow-

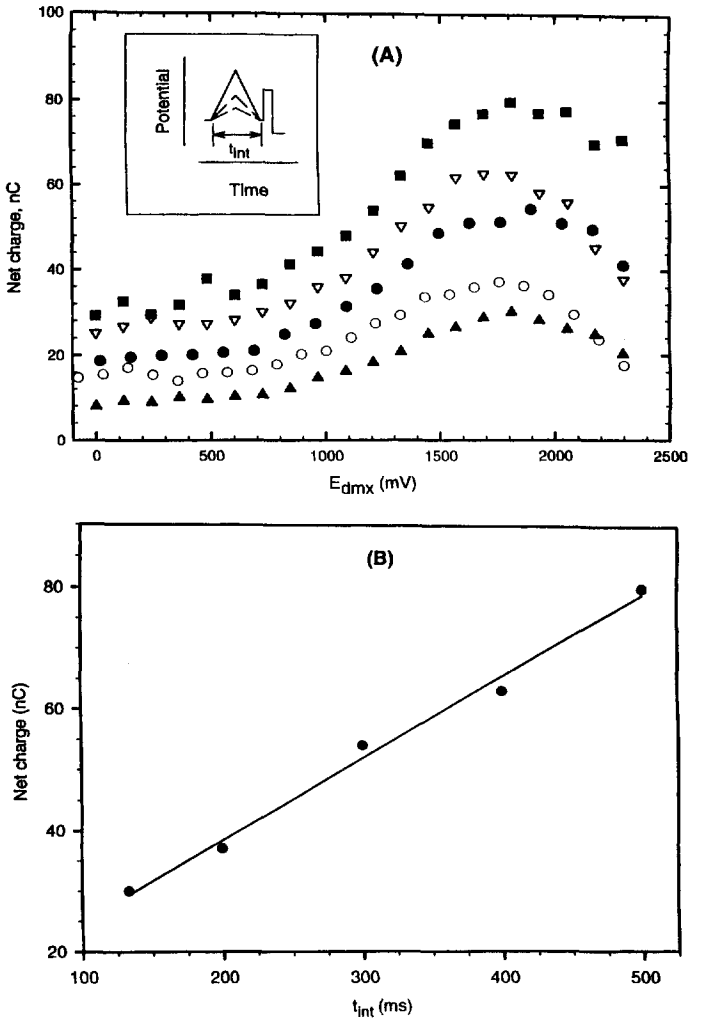

Fig. 4. (A) Pulsed voltammetric background-corrected response as a function of E_{DMX} for dithiane (100 μ*M*) at a 12 μm Au fiber electrode in 10 m*M* phosphate buffer (pH 7.0). The inset shows the scheme of PV optimization. Detection time t_{int} was fixed, E_{dmx} and scan rate were incremented. t_{int} (ms): (■) 500; (▽) 400; (●) 300; (○) 200 and (▲) 133.3. (B) Background-corrected charge maximum as a function of t_{int} (inset: scheme of PV optimization scans).

able value to maintain the integrity of the separation. Similar studies were performed on the IPAD waveform parameters. In a non-deaerated environment, a 30% decrease was observed as the E_{dst} and E_{dnd} were similarly scanned from −400 to −800 mV. Since this same effect was not observed in dearated environments, the effect was attributed to attenuation of the signal from O_2 reduction. E_{dnd} was selected to be −800 mV for aerated and −400 mV for deaerated conditons.

Pulsed voltammetric studies of E_{oxd} and t_{oxd}, which constitute the anodic pulse used to form the "cleaning" oxide, were determined to be +1400 mV and 100 ms, respectively. Over the range of 1400 to 2000 mV, E_{oxd} had no observable effect on the responses of dithiane and GSH. Changing the oxidation period from 50 to 1000 ms resulted in a 10% decrease in signal. These values were chosen to give reliable and effective oxide formation in the least amount of time. Although evidence indicates that the rate of oxidative surface cleaning of the electrode might be accelerated at larger values of E_{oxd}, E_{oxd}= +1500 mV is also chosen to avoid bubble formation from O_2 evolution in the cell.

The surface oxide formed during the application of E_{oxd} in the PAD waveform quickly results in an attenuated electrode response due to the formation of stable surface oxide. E_{red} and t_{red} must be chosen to achieve complete reductive dissolution of the surface oxide. Since the response using PAD at noble metal electrodes is dependent on preadsorption of the analyte, the cathodic polarization step must also be of sufficient duration to allow maximal adsorption of the analyte. In other words, the analyte signal is a function of adsorption kinetics, adsorption isotherm, and the adsorption period. Fig. 5 shows the net charge for GSH and dithiane at reduction potentials of (●) −1100, (■) −675 and (▲) −250 mV. As expected, there is a linear trend up to ca. 1200 ms for both compounds. This effect is directly attributable to a time dependent adsorption component of the total signal. The increase in net charge for a given increment time was measured to be ca. 15% for every additional 200 ms. Since it is imperative that the total waveform time be as small as possible, a choice must be made between the gain in signal from additional adsorption time vs. the gain in signal from addition integration time. Since t_{int} increased by ca. 100% for every 200 ms, t_{red} was selected to be 100 ms and any additional time would be added to the integration period. Table 1 lists the optimal IPAD waveform parameters used for all subsequent studies.

Essential to the use of pulsed voltammetry to optimize IPAD waveforms is that the results agree

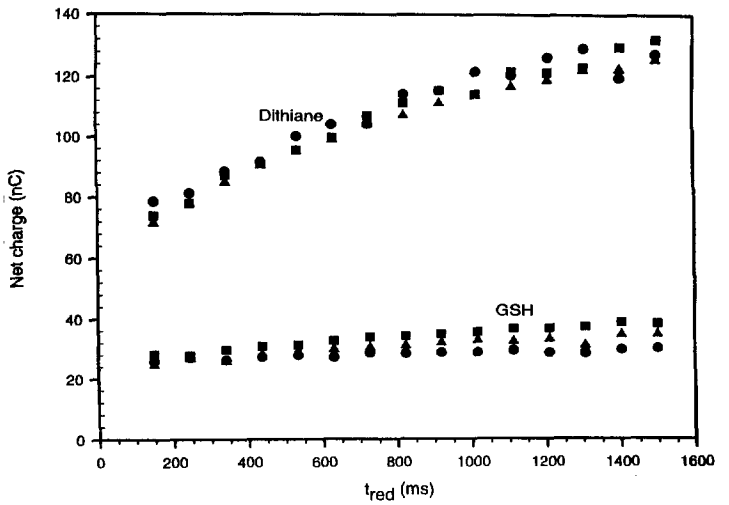

Fig. 5. Pulsed voltammetric background-corrected response for dithiane (100 μ*M*) and GSH (100 μ*M*) as a function of t_{red} and three E_{red} values at a 12 μm Au fiber electrode in 10 m*M* phosphate buffer (pH 7.0). E_{red} (mV): (●) −1100; (■) −675 and (▲) −250.

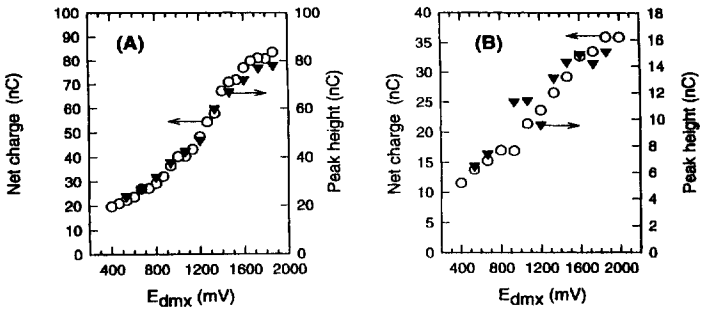

Fig. 6. Comparison of PV response (○) to CE peak heights (▼), as a function of E_{dmx}, for (A) 100 μ*M* dithiane and (B) 100 μ*M* GSH. CE conditions: 11 kV separation voltage, 6 μA current, 10 m*M* pH 7.0 phosphate buffer solution, 50 cm×50 μm I.D., 360 μm O.D. capillary, electrokinetic injection.

with those found for injections on a CE system. As shown in Fig. 6A,B for dithiane and GSH, respectively, the results obtained by the optimization system (○) agrees very well with CE results, which were obtained by repetitive injection of the analyte at different E_{dmx} values. Fig. 7A shows electropherograms obtained for a mixture of dithiane and GSH at various t_{int} values. The nearly linear increase in peak height with an increase in t_{int} shown in Fig. 7B agrees with the results found using pulsed voltammetry, vide infra. The increase in peak height incurs a corresponding increase in *S/N*, which is reflected in a lower limit of detection, Fig. 7B.

3.3. Capillary electrophoresis–IPAD

The separation and detection of cysteine, GSH and GSSG by CE–IPAD is shown in Fig. 8 to illustrate the applicability of IPAD to the direct detection of both thiols and disulfides. This separation was performed at pH 6.3 (Ar-degassed) to avoid on-column oxidation of GSH, which is prevalent at pH>7.0 for

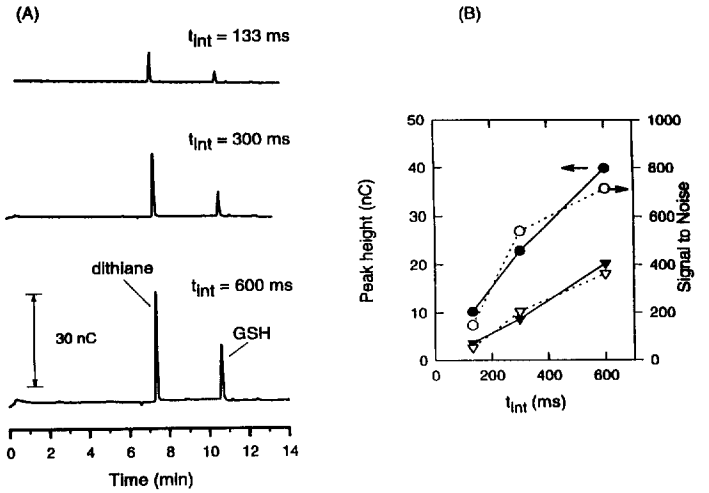

Fig. 7. (A) Electropherograms of a mixture of dithiane and GSH for t_{int} values of 133, 300 and 600 ms. (B) Peak height as a function of t_{int} for dithiane (●) and GSH (▼); and signal-to-noise as a function of t_{int} for dithiane (○) and GSH (▽). CE conditions are the same as for Fig. 6.

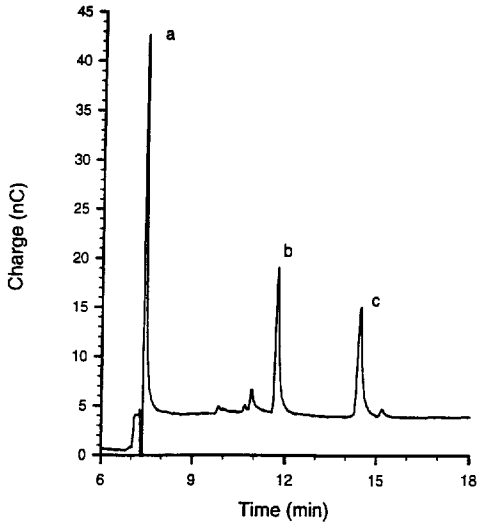

Fig. 8. Electropherogram of a mixture of cysteine, GSH and GSSG in 10 m*M* phosphate buffer, pH 6.3, deaerated with argon. CE conditions are otherwise the same as for Fig. 6. Peaks (100 μ*M* each): (a) cysteine; (b) GSH and (c) GSSG.

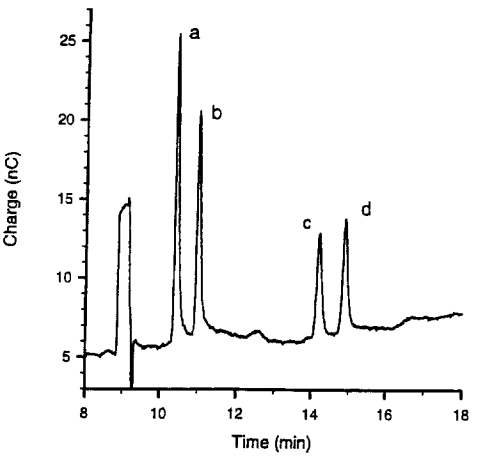

Fig. 9. Electropherogram of a mixture of four antibiotics, amoxicillin, ampicillin, cloxicillin and penicillin-G in 10 m*M* phosphate buffer, pH 7.0. Separation potential 10 kV; CE conditions are otherwise the same as for Fig. 6. Peaks: (a) amoxicillin, 250 μ*M*; (b) ampicillin, 250 μ*M*; (c) cloxacillin, 500 μ*M* and (d) penicillin-G, 500 μ*M*.

concentration less than 10 μ*M*. Table 2 lists the quantitative parameters obtained for this same separation. The limits of detection determined by IPAD for both thiols and disulfides were 0.5 μ*M* (3 fmol); or 0.6, 1 and 2 pg for Cys, GSH and GSSG, respectively, on a mass basis. Regression analysis showed that the responses were linear over 2 decades with good correlation coefficients. Deviations from linearity for calibration plots for thiocompounds are attributable to the preadsorption of the analyte in the detection mechanism, and the extent of deviation directly reflects the strong influence of the analyte's adsorption isotherm. Hence, linear calibration plots can be expected for dilute solutions, and deviations from linearity will occur at higher concentrations, where maximum coverage of the electrode surface is approached. The linearity was improved by a cleaning pulese of $E_{oxd}=1500$ mV and using E_{dst} and E_{dnd} values of −400 mV since there was no advantage in the deaerated environment of the separation.

The response aspects of GSH and dithiane are characteristic of many sulfur-containing compounds. Fig. 9 shows that CE–IPAD is also well suited to the determination of penicillins. Thioethers such as methionine and biotin are detected with ca. one-third the sensitivity as thiols.

Table 2
Quantitative parameters of biologically important thiocompounds at a Au electrode in 10 m*M* phosphate buffer (pH 6.3)

Compound (IPAD)	Linear range $nC=a$ (μ*M*)$+b$				
	LOD[a] (μ*M*, pg)	*a*	*b*	*R*	Range (μ*M*)[b]
Cysteine	0.5, 0.6	1.70	1.42	0.9997	2.5–250
GSH	0.5, 1	1.41	15.5	0.9930	2.5–250
GSSG	0.5, 2	1.40	14.0	0.9968	2.5–250

[a] Limit of detection was calculated at $S/N=3$ from concentrations within five times the LOD.
[b] Linearity was tested below 2.5 μ*M*.

4. Conclusion

Pulsed electrochemical detection following capillary electrophoresis allows for the simple, sensitive and direct detection of numerous thiocompounds. Thiols and disulfides are detected at a single electrode with equal sensitivity. In agreement with past efforts, IPAD is better suited for the universal detection of thiocompounds in CE. Optimization of the IPAD waveform, which need only be done for a particular pH, is facilitated with the use of pulsed voltammetric optimization programs. LODs under optimal conditions are on the order of 0.5 μM (3 fmol) for all compounds tested. Sulfur-containing compounds are selectively detected under mildly acidic conditions., and as a consequence, PED combined with the highly efficient separations of CE offers the analyst direct determination of biologically important compounds with less sample preparation.

Acknowledgments

The authors gratefully acknowledge the discussions and technical assistance of Susan M. Lunte and members of her research group. This work was partially supported by a grant from the Maryland Cancer Program, Dionex Corporation and Special Research Initiative Support from UMBC.

References

[1] D. Voet and J.G. Voet, Biochemistry, Wiley, New York, 1990, p. 709.
[2] A. Larsen, S. Orrenius, A. Holmgren and B. Mannervik, (Editors), Functions of Glutathione, Raven Press, New York, 1983.
[3] A.G. Ewing, J.M. Mesaros and P.F. Gavin, Anal Chem., 66 (1994) 527A.
[4] T.J. O'Shea and S.M. Lunte, Anal. Chem., 65 (1993) 247.
[5] T.J. O'Shea and S.M. Lunte, Anal. Chem., 66 (1994) 307.
[6] B.L. Lin, L.A. Colon and R.N. Zare, J. Chromatogr. A, 680 (1994) 263.
[7] J. Zhou, T.J. O'Shea and S.M. Lunte, J. Chromatogr. A, 680 (1994) 271.
[8] X. Huang and W.Th. Kok, J. Chromatogr. A, 716 (1995) 347.
[9] T.J. O'Shea, S.M. Lunte and W.R. LaCourse, Anal. Chem., 65 (1993) 948.
[10] R.E. Roberts and D.C. Johnson, Electroanalysis, 7 (1995) 1015.
[11] W. Liu and R.M. Cassidy, Anal. Chem., 62 (1993) 2878.
[12] P.L. Weber, T. Kornfelt, N.K. Klausen and S.M. Lunte, Anal. Biochem., 225 (1995) 135.
[13] W.R. LaCourse, Analusis, 21 (1993) 181.
[14] D.C. Johnson and W.R. LaCourse, Electroanalysis, 4 (1992) 367.
[15] D.C. Johnson and W.R. LaCourse, Anal. Chem., 62 (1990) 589A.
[16] W.R. LaCourse and G. S.Owens, Anal. Chim. Acta, 307 (1995) 301.
[17] W.R. LaCourse and D.C. Johnson, Anal. Chem., 65 (1993) 50.
[18] T.J. O'Shea, R.D. Greenhagen, S.M. Lunte, C.E. Lunte, M.R. Smyth, D.M. Radzik and N. Watanabe, J. Chromatogr., 593 (1992) 305.
[19] W.R. LaCourse and G.S. Owens, Electrophoresis, 17 (1996) 310.
[20] W.R. Fawcett, M. Fedurco, Z. Kovácová and Z. Borkowska, J. Electroanal. Chem., 368 (1994) 265.
[21] W.R. Fawcett, M. Fedurco, Z. Kovácová and Z. Borkowska, J. Electroanal. Chem., 368 (1994) 275.
[22] J. Koryta and J. Pradac, J. Electroanal. Chem., 17 (1968) 185.
[23] J. Koryta and J. Pradac, J. Electroanal. Chem., 17 (1968) 177.
[24] J. Pradac and J. Koryta, J. Electroanal. Chem. 17 (1969) 167.
[25] N. Ossendorfova and J. Koryta, J. Electroanal. Chem., 28 (1970) 311.
[26] A.J. Tudos, P.J. Vandeberg and D.C. Johnson, Anal. Chem., 67 (1995) 552.
[27] A.J. Bard and L.R. Faulkner, in Electrochemical Methods, Wiley, New York, 1980, pp. 522, 218.
[28] R. Cordova, M.E. Martins and A.J. Arvia, J. Electrochem. Soc., 126 (1979) 1172.